Desalination and Water Treatment
www.deswater.com
doi: 10.1080/19443994.2015.1087877

57 (2016) 16907–16918
August

Taylor & Francis
Taylor & Francis Group

Mathematical modeling of the Ni(II) removal from aqueous solutions onto pre-treated rice husk in fixed-bed columns: a comparison

Solmaz Saadat[a], Ali Akbar Hekmatzadeh[b], Ayoub Karimi Jashni[a,*]

[a]*Department of Civil and Environmental Engineering, Shiraz University, Shiraz 7134851156, Iran, email: ssaadat@shirazu.ac.ir (S. Saadat), Tel. +98 917 300 7901; Fax: +98 711 6473161; emails: akarimi@shirazu.ac.ir, ajashni@yahoo.ca (A. Karimi-Jashni)*
[b]*Department of Civil and Environmental Engineering, Shiraz University of Technology, Shiraz 7155713876, Iran, email: hekmatzadeh@sutech.ac.ir*

Received 17 May 2014; Accepted 11 August 2015

ABSTRACT

One of the efficient techniques for the removal of heavy metals from wastewater is adsorption. In this paper, the adsorption of Ni on a new porous carbonaceous adsorbent, pre-treated rice husk particles, was investigated in both batch and column experiments. The equilibrium isotherm was described well by both the Langmuir and Freundlich isotherm. The Langmuir constants, q_m and b, were estimated to be 8.0 and 0.15 l/mg, respectively. Different conditions of flow rate, bed heights, and initial nickel concentrations were considered in the column experiments. It was observed that the adsorption capacity of the packed-bed column and the breakthrough time were increased with an increase in the bed height and a decrease in the flow rate and the influent Ni concentration. The traditional Bohart–Adams, Thomas, and Yoon–Nelson models in accompany with the mass transport model were used to describe the adsorption process in the columns. The experimental breakthrough curves were described satisfactorily by all the aforementioned continuous models. However, the predicted maximum adsorption capacity using Bohart–Adams and Thomas models was less than the one obtained from batch equilibrium experiments. Whereas, there was a good agreement between the batch equilibrium results and the continuous mass transport model regarding the maximum adsorption capacity, indicating the prediction of column performance using batch experiments.

Keywords: Pre-treated rice husk; Adsorption; Nickel; Mass transport model; Fixed-bed column

1. Introduction

Heavy metal ions from industrial wastewaters are of environmental concern due to their toxicity, non-biodegradable nature, and accumulation in living organisms. Among heavy metals, nickel is of particular interest because of its stability and toxicological impact on ecosystems and widespread presence in industrial applications [1]. Numerous studies have confirmed the hazardous effects of nickel on human beings' health [2,3]. Effluents containing Ni(II) are widely discharged by many industries [4,5]. Due to the lack of cost-effective treatment alternatives, the safe and effective disposal of nickel-containing

*Corresponding author.

wastewater has become a challenging issue for industries. This issue needs to be addressed.

Biosorption is an alternative heavy metal removal process, which is particularly preferred when natural materials and waste products from industrial and agricultural activities are available in large quantities. Since rice husk is available in large amounts in Iran due to its widespread rice farms, this agricultural by-product was treated with sodium hydroxide to produce a low-cost carbonaceous adsorbent for the removal of nickel ions from aqueous solutions. In this study, rice husk was treated with sodium hydroxide to produce a low-cost carbonaceous adsorbent for the removal of nickel. Although batch laboratory adsorption studies provide useful information regarding the effectiveness of metal-biosorbent systems, in the practical operation of full-scale biosorption, processes continuous-flow columns are required in order to determine the process parameters [6–8]. Several continuous-flow studies have been conducted on the removal of heavy metal in recent years [10–13]. In order to effectively design heavy metal-bearing material units, the development of mathematical models, that can successfully simulate the dynamic behavior of a fixed-bed adsorption column, is required. Researchers have mainly focused on traditional methods, such as Bohart–Adams and Thomas models to describe the dynamic parameters of fixed-bed adsorption columns. However, these models are empirical and based on several simplifications. Although these models are suitable for the data correlation of symmetrical breakthrough curves, they usually fail to describe the performance of packed-bed columns with a complex sorption process, i.e. unsymmetrical breakthrough curves.

To the best of our knowledge, a little attention has been paid to examine the removal of heavy metal in a fixed- bed column packed with biosorbents using the mass transport model without any simplification and its numerical solution. Furthermore, the mass transport model and its numerical solution can be used as a reliable solution to design, optimize, and predict the breakthrough curves of continuous-fixed-bed filters in full-scale industrial wastewater treatment units.

Considering what has been discussed so far, the first objective of this study was to evaluate the effects of bed height, initial Ni concentration, and flow rate on the removal of Ni(II) ions by NaOH-treated rice husk. The second objective was to develop a mathematical model, mass transport model, including advection, dispersion, and adsorption terms to describe the breakthrough curves. The experimental breakthrough data were also fitted to the Yoon–Nelson, Thomas, and Bohart–Adams models to estimate the associated parameters and subsequently compare the suitability of the aforementioned models. Furthermore, a sensitivity analysis was conducted to determine how the different values of models' parameters affect the shape of breakthrough curve.

2. Materials and methods

2.1. Preparation of pre-treated rice husk adsorbent

The rice husk used in these experiments was obtained from a local rice mill. It was washed several times with distilled water to remove dust and other impurities. In order to extract soluble organic compounds from the rice husk, 15 g of dried rice husk was treated with 150 mL of 1.0 M NaOH in a shaker for 24 h [14]. The mixture was filtered and washed again several times with distilled water to remove excess NaOH from the treated rice husk. Afterward, it was left to dry at room temperature for 24 h [13].

2.2. Reagents

All chemicals used for the study were of analytical reagent grade. A stock solution of Ni(II) (1,000 mg/L) was prepared by dissolving a specified amount of $NiSO_4$ in distilled water. The solution was then diluted to the desired concentrations for the experiments. The initial pH of the working solution was adjusted to 7 by adding HCl or NaOH solutions.

2.3. Batch experiments

In the batch equilibrium experiments, a measured quantity of the pre-treated rice husk was added to a series of 250 mL glass bottles containing Ni(II) solutions with different concentrations. The bottles were rotated for 24 h at 25°C in a temperature-controlled rotating shaker. After equilibration, the slurry was filtered and the concentration of the supernatant was measured using an atomic absorption spectrophotometer (Shimadzu A-A 680). The amount of Ni(II) adsorbed onto the adsorbent was then calculated via mass balance. In addition, batch kinetic tests were carried out to determine the equilibrium time. In these tests, the bottles were withdrawn from the shaker at predetermined time intervals to measure their Ni concentrations. It should be noted that all experiments were performed in triplicate.

2.4. Fixed-bed column adsorption studies

Column experiments were performed in a glass column with an internal diameter of 3.6 cm and a length of 100 cm. A schematic diagram of the

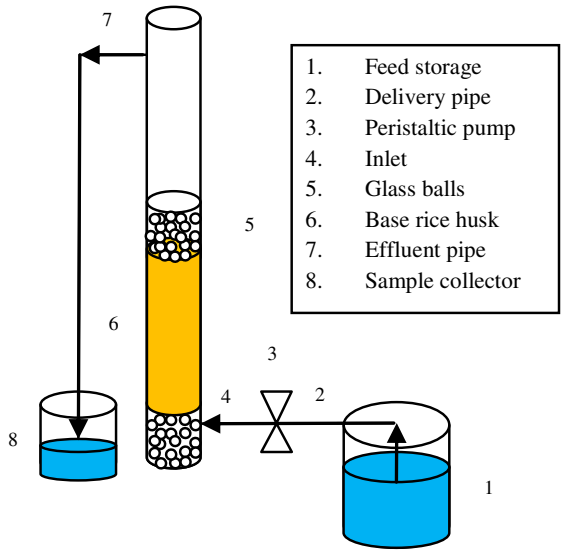

Fig. 1. Experimental setup for fixed-bed column study.

column experimental setup used for the fixed-bed tests is shown in Fig. 1. The column was packed with adsorbent between two supporting layers of glass beads. The experiments were carried out at a room temperature of 25 ± 1°C. The nickel solution was passed through the column bed at a certain concentration in an upward direction to ensure a completely saturated bed and to avoid the possibility of short-circuiting and channeling [15,16]. A peristaltic pump was used to maintain a constant flow rate during the experiments. A total of seven experiments were carried out at different conditions of flow rate, bed depth, and influent Ni(II) concentration. The characteristics of these experiments are given in Table 1. Samples from the column effluent were collected every 5–15 min at the early stage of the experiment and it was increased to every 30 min at the late stages of the experiments. Samples were analyzed for Ni concentration using the atomic absorption spectrometer. The measurements were performed in triplicate and the average values are presented. The pH was kept constant at 7 for all experiments. It should be noted that the effluent pH was continuously recorded. Moreover, the porosity and the bulk density of the packed-bed column were determined as 0.75 and 73.6 mg/L, respectively.

2.5. Mass transport model

The concentration-time profile through an adsorption column can be described by applying the mass balance of solute in a differential segment of a column, which is shown by the following advection-dispersion equation:

Table 1
Measured characteristic of column tests and model parameter predictions

Continuous no.	Run 1	Run 2	Run 3	Run 4	Run 5	Run 6	Run 7
Q (ml/min)	17.5	17.5	17.5	17.5	17.5	13.25	9.0
H (cm)	30	20	10	20	20	20	20
C (mg/L)	51	45	47.5	87.5	17	55	51
Rice husk mass (g)	22.5	15	7.5	15	15	15	15
Adsorption capacity (mg Ni/mg adsorbent)	6.1	4.2	2.6	3.5	4.6	5.2	5.6
Mathematical model parameters							
q_m (mg/g)	8.5	7.1	7.3	7.0	8.1	7.2	8.0
b (L/mg)	0.06	0.05	0.05	0.02	0.085	0.07	0.07
D (m^2/s) × 10^5	11.0	8.0	11.0	10.0	7.5	9.5	12.0
R^2	0.972	0.980	0.954	0.953	0.963	0.987	0.983
Bohart–Adams parameters							
q_m (mg/g)	5.9	4.5	4.0	4.1	4.4	4.8	5.0
k_{qu} (L/mg h)	0.034	0.051	0.048	0.028	0.055	0.032	0.031
R^2	0.981	0.990	0.973	0.976	0.984	0.991	0.992
Thomas parameters							
q_m (mg/g)	6.0	5.5	4.1	4.1	6.0	5.0	5.2
b (L/mg)	0.1	0.05	0.1	0.06	0.13	0.14	0.11
k_{kin} (L/mg h)	0.033	0.048	0.045	0.023	0.046	0.03	0.031
R^2	0.983	0.991	0.973	0.977	0.984	0.992	0.993

$$\frac{\partial(C)}{\partial t} = D\left(\frac{\partial^2 C}{\partial x^2}\right) - u\frac{\partial C}{\partial x} - \frac{\rho_b}{\varepsilon_b}\frac{\partial \bar{q}}{\partial t} \quad (1)$$

where C is the Ni(II) concentration in the column void, $\bar{q}$ is the Ni(II) concentration on the solid phase, u stands for the pore velocity, D represents the axial dispersion, and ρ_b and ε_b are the bulk density and the bed porosity of the packed adsorbents, respectively. According to the experimental setup, the initial and boundary conditions of Eq. (1) are stated through relations 2–4:

$$C(0,t) = C_0 \quad 0 \le t \quad (2)$$

$$C(x,0) = 0 \quad (3)$$

$$C(x \to \infty, t) = 0 \quad (4)$$

where C_0 is the inlet nickel concentration. Eq. (1) contains two known parameters, C and q. Consequently, one more relationship between C and q is required in order to obtain the solution of this equation. Assuming local equilibrium between nickel concentration in liquid and solid phases, the Langmuir isotherm, Eq. (5), can provide a relationship between C and $\bar{q}$.

$$\bar{q} = \frac{bq_m C}{1 + bC} \quad (5)$$

Furthermore, the adsorption term in Eq. (1), $\partial\bar{q}/\partial t$, can be replaced with the following equation:

$$\frac{\partial \bar{q}}{\partial t} = \frac{\partial \bar{q}}{\partial C}\frac{\partial C}{\partial t} \quad (6)$$

By taking partial differentiation of Eq. (5), the following relation is obtained:

$$\frac{\partial \bar{q}}{\partial C} = \frac{bq_m}{(1 + bC)^2} \quad (7)$$

The combination of Eqs. (1), (5), (6), and (7) gives the governing mass balance equation (Eq. (8)) in a column packed with adsorbent particles:

$$\left(1 + \frac{\rho_b}{n}\frac{bC}{(1 + bC)^2}\right)\frac{\partial C}{\partial t} = D\frac{\partial^2 C}{\partial x^2} - u\frac{\partial C}{\partial x} \quad (8)$$

2.5.1. Numerical solution of mass transport model

Eq. (8) can be solved using numerical techniques, such as finite difference method. The governing equation, Eq. (8), was converted to a set of algebraic equations using the Crank–Nicolson scheme, which is an implicit finite difference method. The algebraic form of Eq. (8) can be expressed as follows:

$$R_i^n\frac{C_i^{n+1} - C_i^n}{\Delta t} = \frac{D}{(\Delta x)^2}\left(\frac{(C_{i+1}^n - 2C_i^n + C_{i-1}^n) + (C_{i+1}^{n+1} - 2C_i^{n+1} + C_{i-1}^{n+1})}{2}\right) + \frac{u}{\Delta x}\left(\frac{(C_{i+1}^n - C_{i-1}^n) + (C_{i+1}^{n+1} - C_{i-1}^{n+1})}{2}\right) \quad (9)$$

This numerical technique has a second-order temporal truncation error, resulting in a higher accuracy of solutions. In addition, numerical dispersion is zero and, consequently, the estimated dispersion coefficient is not affected by the discretization of the domain [17]. The aforementioned algebraic equations were solved using a computer code in MATLAB program.

2.6. The Thomas model

The Thomas model, derived in 1944, is one of the widely recognized analytical solutions of Eq. (1). This model assumes that the axial dispersion is negligible and the adsorption term, $\partial\bar{q}/\partial t$, can be stated as the following second-order reaction rate relation [18,19]:

$$\frac{d\bar{q}}{dt} = k_{kin}\left[C(q_m - \bar{q}) - \frac{\bar{q}}{b}\right] \quad (10)$$

where k_{kin} is the specific rate factor for adsorption, q_m is the maximum adsorption capacity, and b is the Langmuir constant. At equilibrium ($d\bar{q}/dt = 0$), Eq. (10) essentially becomes the Langmuir isotherm:

$$\overline{q} = \frac{bq_{\mathrm{m}}C}{1+bC} \tag{11}$$

If the axial dispersion is ignored, the analytical solution to Eq. (1) can be stated as follows:

$$\frac{C}{C_0} = \frac{J(rs,T)}{J(rs,T) + e^{(r-1)(T-s)}[1-J(s,rT)]} \tag{12}$$

where J is a function expressed as Eq. (13). r, s, and T are the dimensionless coefficients, stated through Eqs. (14)–(16).

$$J(x,y) = 1 - \int_0^x e^{-y-\xi} I_0\left(2\sqrt{y\xi}\right) d\xi \tag{13}$$

$$r = \frac{1}{1+bC_0} \tag{14}$$

$$T = K_{\mathrm{kin}}\, C_0\, \frac{q_{\mathrm{m}}}{q_0} \left(t - \frac{V_{\mathrm{bed}}\, \varepsilon_{\mathrm{b}}}{Q}\right) \tag{15}$$

$$s = \frac{T\, q_0\, \rho_{\mathrm{b}}\, V_{\mathrm{bed}}}{C_0\,(tQ - V_{\mathrm{bed}}\, \varepsilon_{\mathrm{b}})} \tag{16}$$

$$q_0 = \frac{bC_0q_{\mathrm{m}}}{1+bC_0} \tag{17}$$

In the above relations, I_0 is the modified Bessel function of the first kind, Q and V_{bed} are the flow rate and the adsorbent bed volume, respectively. q_0 is the capacity of adsorbent at equilibrium time, defined by Eq. (17). The evaluation of function J is mathematically complicated due to integral over the Bessel function. This function can be estimated using the following mathematical approximation when the product of x and y is greater than 36:

$$J(x,y) = \frac{1}{2}\left\{1 - erf\left(\sqrt{x} - \sqrt{y}\right) + \frac{e^{-(\sqrt{x}-\sqrt{y})^2}}{\sqrt{\pi}\left(\sqrt{y} + \sqrt[4]{xy}\right)}\right\} \tag{18}$$

2.7. The Bohart–Adams model

The Bohart–Adams model is based on surface reaction rate theory. Considering Eq. (1), the adsorption term in this equation is described by a quasi-chemical kinetic rate expression [20]:

$$\frac{\mathrm{d}\,\overline{q}}{\mathrm{d}t} = k_{\mathrm{qu}}\left[C\left(q_{\mathrm{m}} - \overline{q}\right)\right] \tag{19}$$

where k_{qu} is the quasi-chemical rate constant. This kinetic relation is converted to the rectangular isotherm at equilibrium state.

$$\overline{q} = q_{\mathrm{m}} \tag{20}$$

The analytical solution of Eq. (1) in conjunction with Eq. (19), not considering the axial dispersion, is shown in:

$$\frac{C_{\mathrm{b}}}{C_0} = \frac{e^{\alpha}}{e^{\alpha} + e^{\beta} - 1} \tag{21}$$

$$\alpha = k_{\mathrm{qu}}C_0\left(t - \frac{L}{u}\right) \tag{22}$$

$$\beta = \frac{k_{\mathrm{qu}}\rho_{\mathrm{b}}q_{\mathrm{m}}L}{u\varepsilon_{\mathrm{b}}} \tag{23}$$

2.8. The Yoon–Nelson

The Yoon–Nelson model is a simple equation addressing the adsorption process in column. This model requires less detailed data regarding the physical properties of the column and the characteristic of the adsorbent [21,22]. Yoon–Nelson equation is stated as below:

$$\frac{C}{C_0} = \frac{\exp(K_{\mathrm{YN}}\, t - \tau\, K_{\mathrm{YN}})}{1 + \exp(K_{\mathrm{YN}}\, t - \tau\, K_{\mathrm{YN}})} \tag{24}$$

In this equation, K_{YN} is the Yoon–Nelson rate constant; and τ represents the half-breakthrough time. The linear form of the above equation is expressed as follows:

$$\ln\frac{C}{C_0 - C} = K_{\mathrm{YN}}\, t - \tau\, K_{\mathrm{YN}} \tag{25}$$

Therefore, the model constant K_{YN} and τ can be obtained from the plot of $\ln C/C_0 - C$ vs. time t.

2.9. Parameters estimation

In order to obtain the constants of the models introduced here, an objective function, defined as the root mean square of errors (RMSE) between the

experimental data and the model predictions, was minimized:

$$\mathrm{RMSE} = \sqrt{\frac{\sum_{i=1}^{n} \left(C_{\mathrm{exp},i} - C_{\mathrm{model},i}\right)^2}{n}} \tag{26}$$

where C_{exp} and C_{mod} are the experimental and model predictions of Ni(II) concentration, respectively. The "lsqnonlin" function in the optimization toolbox of MATLAB program was employed to determine the values of the model parameters.

3. Results and discussion

3.1. Batch experiments results

Fig. 2 shows the time decay profile of Ni removal using the pre-treated rice husk. As depicted, the majority of Ni removal (83 percent) occurred in the first 15 min, indicating the fast rate of adsorption in the initial minutes. However, the adsorption rate gradually decreased until reaching the state of equilibrium. Although the state of complete equilibrium was achieved at 240 min, the adsorption process was close to equilibrium phase after 60 min.

The adsorption process involves the transport of pollutants through the liquid film surrounding the adsorbent particles, followed by their diffusion into the interior pores. Consequently, the rate of adsorption process may be controlled by the diffusion through the particles and the liquid film around them. The possibility of film diffusion, or intraparticle diffusion, or both was inspected using the Weber and Morris model [23,24], stated as Eq. (27).

$$q = c + k_{\mathrm{i}}\, t^2 \tag{27}$$

where k_{i} is the intraparticle diffusion rate constant and c is the intercept of the vertical axis. According to Eq. (27), the intraparticle diffusion will be the rate-controlling mechanism if the plot of the square root of time vs. the uptake (q) gives a straight line. Otherwise, both film and intraparticle diffusion are rate-limiting mechanisms. As shown in Fig. 3, the above-mentioned plot represents multi-linearity with separate region, indicating the contribution of different diffusion mechanisms including film and intraparticle diffusion. Similar results were observed for the removal of copper by low-cost biosorbents performed by Cochrane et al. [23].

The Langmuir isotherm is a widely used model in the literature for describing the equilibrium data. The model assumes that the adsorption occurs in a finite number of sites with no lateral interactions between neighboring adsorbed molecules. Eq. (28) represents the linear form Langmuir isotherm:

$$\frac{1}{q} = \frac{1}{k q_{\mathrm{m}} C} + \frac{1}{q_{\mathrm{m}}} \tag{28}$$

The batch equilibrium data for the adsorption of Ni(II) onto the pre-treated rice husk are depicted in Fig. 4. In this figure, the solid line represents a description of

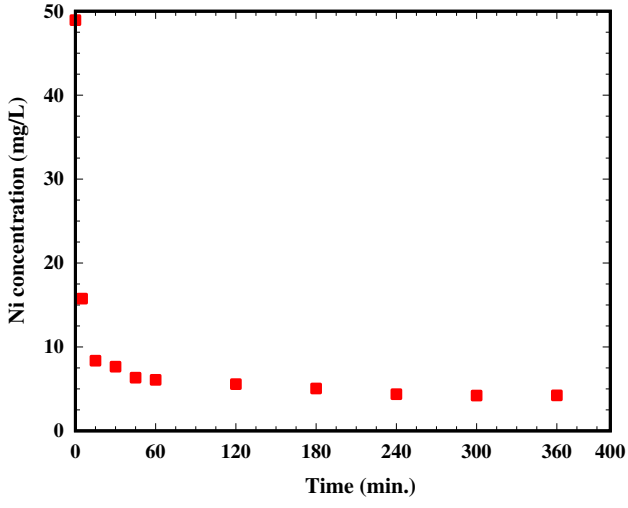

Fig. 2. Experimental time profiles of Ni adsorption onto the adsorbent.

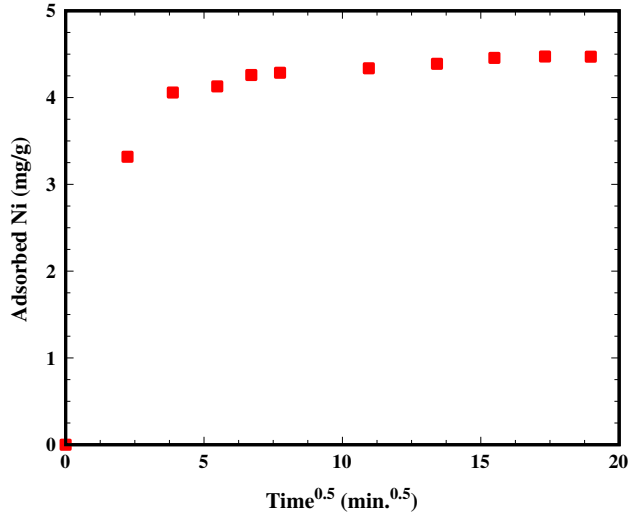

Fig. 3. Intraparticle diffusion kinetics of Ni.

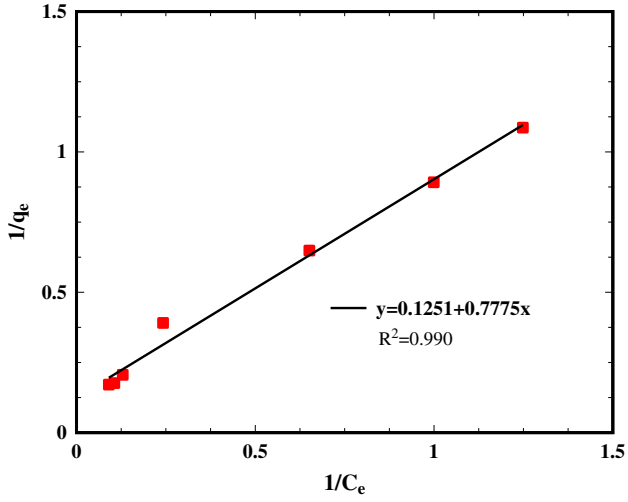

Fig. 4. Langmuir isotherm plot for the removal of Ni(II) on pre-treated rice husk.

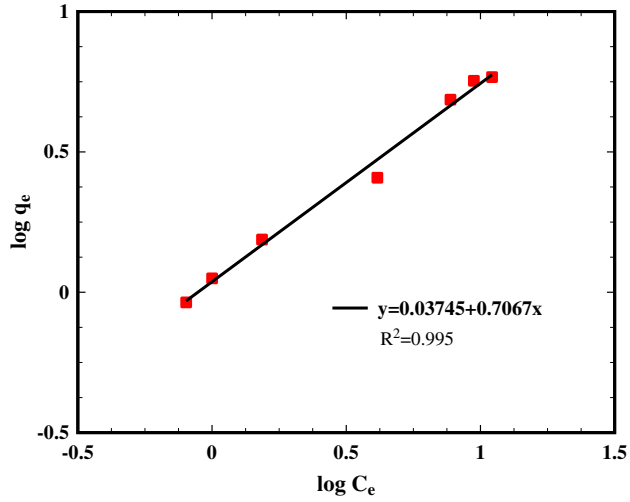

Fig. 5. The Freundlich isotherm plot for the removal of Ni(II) on pre-treated rice husk.

the equilibrium data in terms of the linear form of Langmuir equation (Eq. (28)). As can be seen, there is a good agreement between the predicted line and the experimental data, indicating a satisfactory description of isotherm data using the Langmuir isotherm. The correlation coefficient of 0.99 confirms the adequate fit of the Langmuir model to the experimental data. The isotherm constants, q_m and b, were estimated to be 8.0 and 0.15 l/mg, respectively, using linear regression.

The equilibrium experimental data were also modeled using the Freundlich isotherm illustrating the sorption process onto heterogeneous surface. Eq. (29) indicates the logarithmic form of the Freundlich isotherm.

$$\log q = \log k_f + \frac{1}{n} \log C \tag{29}$$

where k_f and n are Freundlich constants, respectively. According to Fig. 5, the isotherm is fitted to experimental data appropriately with the correlation coefficient of 0.99. The values of k_f and n were determined as 1.09 mg/g and 1.42, respectively. It should be pointed out that the values of n between 1 and 10 indicate the condition of a favorable adsorption.

3.2. Column experiments results

Seven column experiments were carried out at divers operating condition including flow rate, initial concentration, and bed height. The characteristics of these experiments are given in Table 1.

3.2.1. Effect of bed depth (adsorbent mass)

The effect of bed height on the adsorption performance was examined using column tests Run 1, Run 2, and Run 3 (Fig. 6(a)). As the bed height increased from 10 to 30 cm, the adsorption capacity of the columns raised from 2.6 to 6.1 mg-Ni/mg-adsorbent. In addition, by increasing bed height, breakthrough time (time related to $C/C_0 = 0.9$) was also augmented. The reason for this is that Ni(II) ions have more time to make contact with the pre-treated rice husk at a higher bed depth. Furthermore, the slope of breakthrough curve decreased as the adsorbent mass increased, resulting in an expanded mass transfer zone. The increase in the removal of heavy metal along with adsorbent mass is due to the increase in the surface area of the adsorbent, which provides more binding sites for adsorption. A similar trend has been observed by many researchers [25–27] when different biosorbent materials are used in the removal of heavy metals.

3.2.2. Effect of inlet Ni(II) concentration

The adsorption performance of NaOH-modified rice husk was investigated by different Ni(II) influent concentrations ranging from 17 to 88 mg/L (Runs 2, 4, 5). The results showed that the adsorption process reached saturation earlier as the inlet Ni(II) concentration increased (Fig. 6(b)). Fig. 6(b) also shows that breakthrough time decreased as the influent concentration increased. Moreover, the adsorption capacity slightly increased from 3.5 to 4.6 mg-Ni/mg-adsorbent by

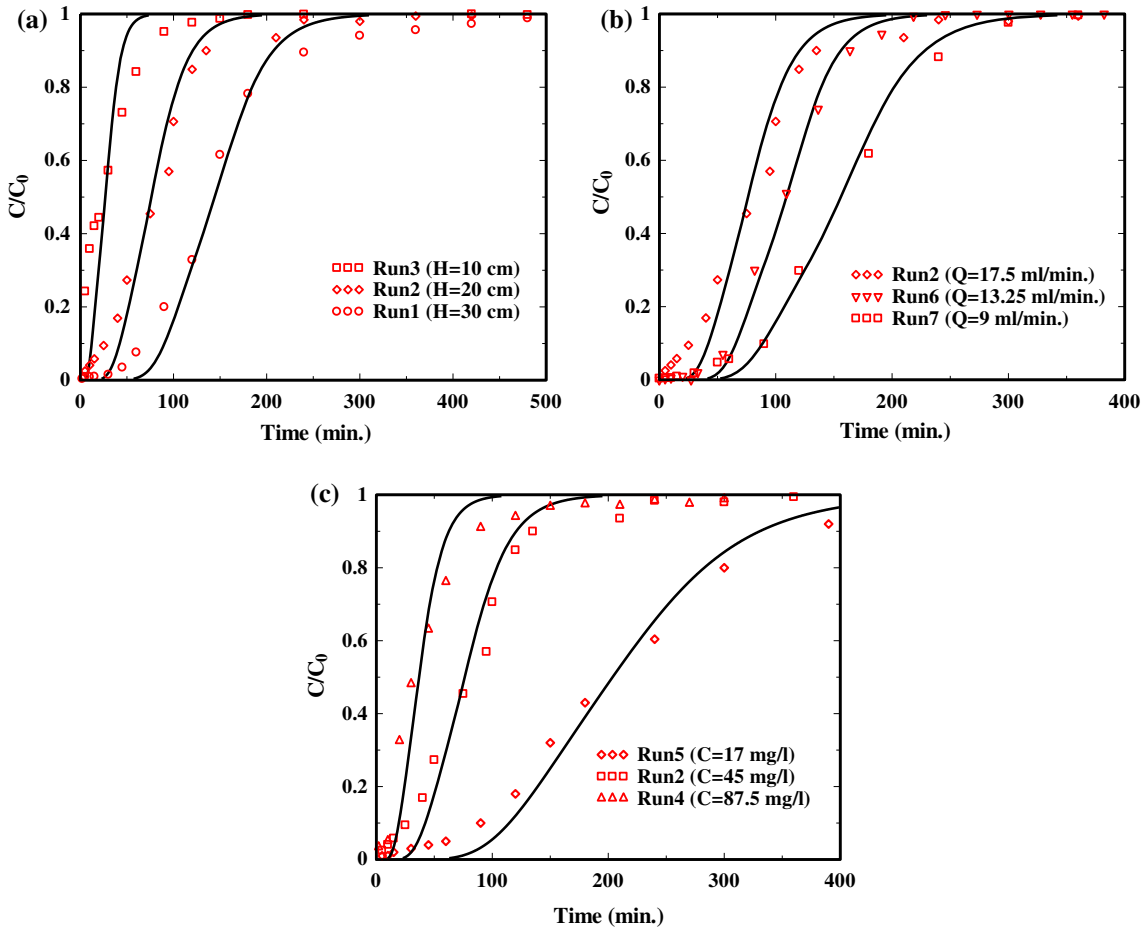

Fig. 6. Measured and modeled breakthrough curves (based on mass balance model) of Ni(II) ions at different (a) bed depths, (b) flow rates, and (c) initial Ni(II) concentrations.

decreasing the influent concentration. In addition, the treated volume was the greatest at the lowest influent concentration. Similar results can be seen in studies carried out in this area [28,29].

3.2.3. Effect of flow rate

The effect of flow rate on the adsorption behavior of Ni(II) onto pre-treated rice husk columns was examined at the flow rates of 9, 13.25, and 17.5 mL/min (Runs 2, 6, 7). As the flow rate increased from 9 to 17.5 mL/min, the breakthrough time and the adsorption capacity decreased from 300 to 150 min and 5.6 to 4.2 mg-Ni/mg-adsorbent, respectively (Fig. 6(c)). At higher flow rates, the external film mass resistance at the surface of the adsorbent tends to decrease and the residence time declines, leading to a drop in saturation time [23]. Furthermore, the breakthrough curve became steeper as the flow rate increased. This is due to the fact that at higher flow rates, Ni(II) ions did not have enough time to make contact with NaOH-modified rice husk, which resulted in a lower removal of Ni(II) in the column.

3.3. Breakthrough curve modeling

The adsorption dynamics of Ni(II) with the pre-treated rice husk in fixed-bed columns were examined using the mass transport model alongside Thomas, Bohart–Adams, and Yoon–Nelson models. The experimental breakthrough data were satisfactorily described by all aforementioned models.

As depicted in Fig. 6, there is a good agreement between the experimental breakthrough curves under different operating conditions and the predictions using the mass transport model. High values of correlation coefficient ($R^2 > 0.95$) confirm the suitability of the proposed mathematical model for describing

the adsorption process through the column. The isotherm constants, b and q_m, and the axial dispersion coefficient, D, are the main unknown constants of the mass transport model (Eq. (8)). These parameters were estimated by minimizing the errors between the experimental breakthrough curves and the mathematical model predictions. The estimated values of q_m for all column experiments, ranging from 7 to 8.5 mg/g, are close to the average value (7.6 mg/g). In addition, the Langmuir constants, b, were found to be between 0.02 and 0.07, which are relatively close to each other. The small differences in the estimations of q_m and b are probably due to the variations in the empty bed contact time (EBCT) and the initial Ni(II) ion concentrations. This may be explained by the fact that the retention time is not sufficient to reach complete equilibrium in column tests with a lower EBCT.

It is worth mentioning that the isotherm constants estimated from batch and continuous experiments indicate a reasonably satisfactory degree of agreement. The average value of the maximum adsorption capacity, q_m, estimated by the mathematical model for column experiments (7.6 mg/g), is very close to the value determined in the batch process (8.0 mg/g). Consequently, the results of batch experiments can be used for modeling of the adsorption process in the continuous bed.

The difference in the values of the isotherm constant, b, found in the batch and continuous experiments can be attributed to the fact that the complete equilibrium may have not been established in the bed, resulting in the smaller Langmuir constant b. A similar observation was reported by Selvaraju and Pushpavanam [30]. They investigated the adsorption of nitrate, chloride, phosphate, and surfactant onto sand and brick particles, which leads to a smaller Langmuir constant, b, in the column experiments.

The dispersion coefficient was computed in the range of 7×10^{-5}–12×10^{-5} m^2/s. It should be noted that there are several methods for estimating the dispersion coefficient, such as the well-known Chung and Wen formula [31]. Nonetheless, these methods are typically applied to spherical activated carbon and not pre-treated rice husk particles with their boat-like shape.

Considering the Bohart–Adams and Thomas models, the values of the correlation coefficient, R^2, are higher than 0.97, which indicate a satisfactory description of each set of columns data by these models (Table 1). For the sake of brevity, the high level of agreement between the four column breakthrough curves and the predictions using Thomas model is shown in Fig. 7. Similar results were obtained by applying Bohart–Adams model to the

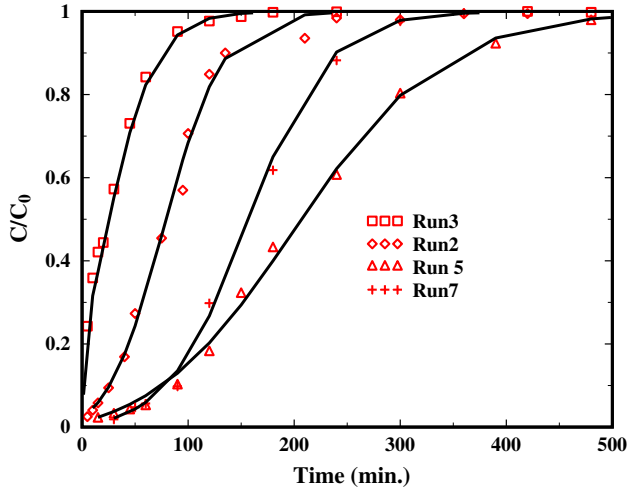

Fig. 7. Measured and modeled breakthrough curves (based on Thomas model) of Ni(II) ions for 4 column tests.

experimental data. The specific adsorption rate factor (k_{kin}) in addition to Langmuir constants, q_m and b, are the three unknown coefficients of the Thomas model, whereas the Bohart–Adams equation has only two unknown factors: (1) the maximum adsorption capacity (q_m) and (2) quasi-chemical rate constant (k_{qu}). The estimations of these parameters for all experiments are presented in Table 1. The maximum adsorption capacity and the adsorption rate factor for all experiments are highly close to each other. The values of k_{qu} and k_{kin} are in the range of 0.028 to 0.055 and 0.023 to 0.048 L/mg min, respectively. The small differences between the estimations of k_{qu} and k_{kin} can be explained by assuming rectangular isotherm in the Bohart–Adams model, whereas the Langmuir isotherm was employed in the Thomas model. In addition, the values for maximum adsorption capacity, q_m, were approximated in the range of 4.0–6.0 mg/g, which are highly smaller than those obtained using mass transport model or bath isotherm data. This is due to the fact that the axial dispersion is neglected in the Bohart–Adams and Thomas models, while these models are able to predict the shape of breakthrough curves satisfactorily. It is important to note that the slope of breakthrough curve is influenced considerably by axial dispersion. Accordingly, it is deduced that the constants of Thomas and Adam-Bohart models (K_{ch}, k_{kin}, and q_m) are empirical and include the effect of axial dispersion.

The column breakthrough curves were also described by the Yoon–Nelson relation. The constants of this model, K_{YN} and τ, were determined by the linear plot of $\ln(C/(C_0 - C))$ vs. time t with relatively

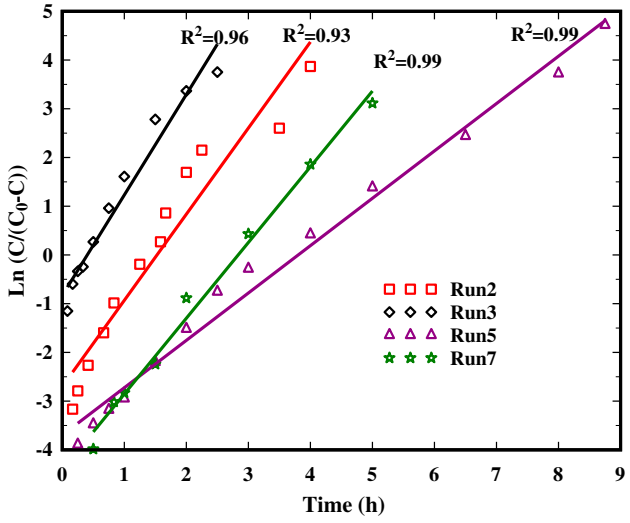

Fig. 8. Liner plot of the Yoon–Nelson model for 4 column tests.

high linearized correlation coefficients ranging from 0.93 to 0.99. For the sake of brevity, four linear plots are depicted in Fig. 8. The aforementioned constants and the corresponding linear correlation coefficients are tabulated in Table 2. The model predictions exhibited a satisfactory match to the experimental breakthrough curves as shown in Fig. 9. Moreover, as seen in Table 2, the predicted 50 percent breakthrough time, τ, is close to the experimental ones, confirming the suitability of this model for describing the column data. It was also observed that the rate constant, K_{YN}, increased with a decrease in bed height.

3.4. Sensitivity analysis

Sensitivity analysis was performed in order to investigate the effect of model parameters on the prediction of column breakthrough curves. The column test Run 1 with an initial concentration of 47.5, a bed height of 30 cm, and a solution discharge of 17.5 L/s were selected for this purpose. Fig. 10 shows the result of the sensitivity analysis carried out on the predictions obtained using mass transport model. The variations in the isotherm parameters, q_m and b, caused a shift in the breakthrough time.

However, the shape of the breakthrough curves was not affected considerably. Additionally, according to Fig. 10(c), a change in the value of dispersion coefficient, D, caused both the breakthrough time and the slope of breakthrough curve to change, indicating the sensitivity of the mass transport model to this coefficient. The sensitivity of Thomas model to the model parameters was also investigated, as shown in Fig. 11. The slope of breakthrough curve is altered by variations in the value of the specific rate factor (k_{kin}). However, the total adsorption capacity of the column is nearly the same for different values of k_{kin}. Furthermore, the larger the specific rate factor is, the steeper the breakthrough curve is. Finally, similar to what obtained for the mass transport model, the breakthrough point moved as a result of changes in the values of the Langmuir constants, q_m and b, which, for the sake of brevity, relevant figures are not shown here. Comparable sensitivity results were also obtained for the Bohart–Adams model.

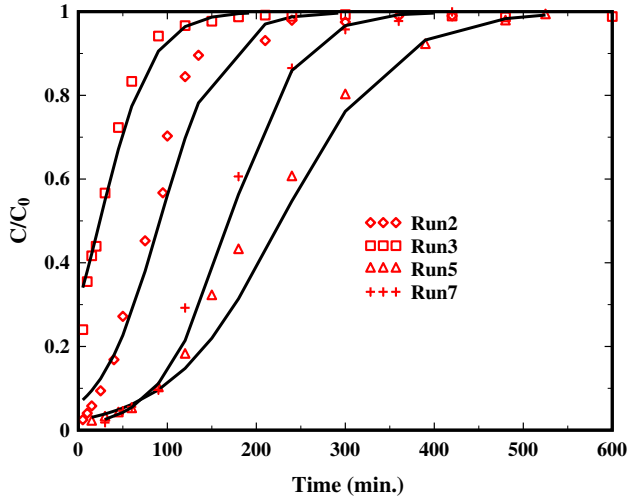

Fig. 9. Measured and modeled breakthrough curves (based on Yoon–Nelson model) of Ni(II) ions for 4 column tests.

Table 2
Model parameters of Yoon–Nelson model

Column no.	Run 1	Run 2	Run 3	Run 4	Run 5	Run 6	Run 7
K_{YN}	1.59	1.77	2.06	1.87	0.97	2.55	1.55
τ cal.	2.70	1.53	0.40	0.51	3.80	1.88	2.84
τ exp.	2.31	1.39	0.41	0.53	3.40	1.82	2.66
Linearized R^2	0.939	0.928	0.961	0.962	0.987	0.978	0.990

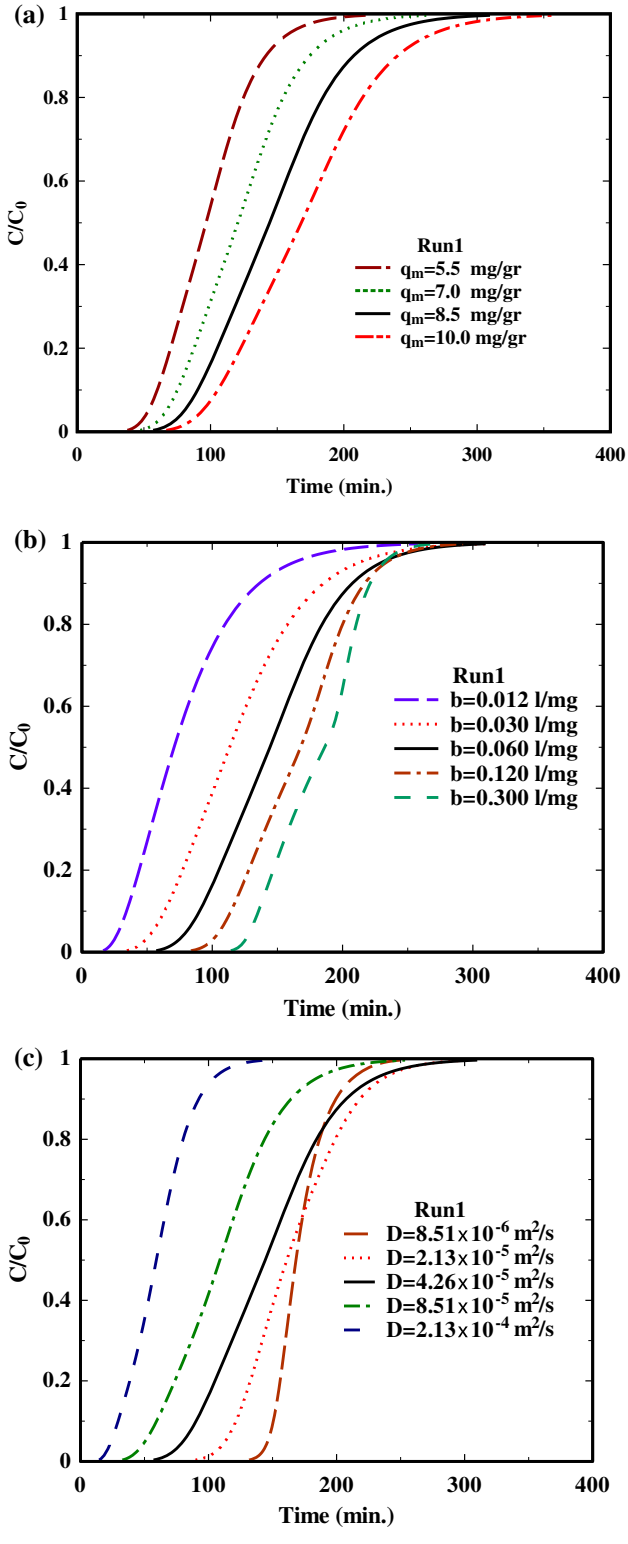

Fig. 10. Effect of variation in the parameters of the mass balance model on the breakthrough profile based on column test Run 1: (a) maximum adsorption capacity, q_m. (b) Langmuir constant, b. and (c) dispersion coefficient, D.

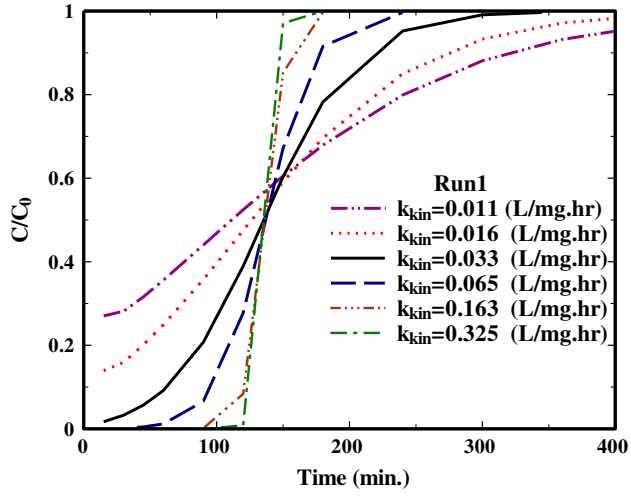

Fig. 11. Effect of variation in the specific rate factor for adsorption on the breakthrough profile based on column test Run 1.

4. Conclusions

The adsorption of Ni on a new porous carbonaceous adsorbent was investigated in both batch and column tests. The removal of Ni(II) through the column was dependent on bed depth, influent concentration, and flow rate. The adsorption capacity of the packed-bed column and the breakthrough time increased with an increase in bed height, a decrease in flow rate and influent Ni concentration. The batch equilibrium data were described appropriately by both Langmuir and Freundlich isotherms. The Langmuir constants, q_m and b, were estimated to be 8.0 and 0.15 l/mg, respectively. Both mass transport model and traditional models, such as Bohart–Adams, Thomas, and Yoon–Nelson models, satisfactorily describe the experimental data. Nevertheless, the maximum adsorption capacity estimated by the mass transport model (7.6 mg/g) is more in accordance with the results of batch experiments, indicating the ability of the proposed model to predict column behavior using batch results. The results of sensitivity analysis showed that changes in the Langmuir isotherm lead to changes in the breakthrough point in the presented continuous models.

Acknowledgment

The authors would like to acknowledge Fars Province Water and Wastewater Co. for their partial support of this project.

References

[1] H. Javadian, P. Vahedian, M. Toosi, Adsorption characteristics of Ni(II) from aqueous solution and industrial wastewater onto Polyaniline/HMS nanocomposite powder, Appl. Surf. Sci. 284 (2013) 13–22.

[2] C. Quintelas, R. Pereira, E. Kaplan, T. Tavares, Removal of Ni(II) from aqueous solutions by an *Arthrobacter* viscosus biofilm supported on zeolite: From laboratory to pilot scale, Bioresour. Technol. 142 (2013) 368–374.

[3] C. Valderrama, J.A. Arévalo, I. Casas, M. Martínez, N. Miralles, A. Florido, Modelling of the Ni(II) removal from aqueous solutions onto grape stalk wastes in fixed-bed column, J. Hazard. Mater. 174 (2010) 144–150.

[4] R. Sharma, B. Singh, Removal of Ni(II) ions from aqueous solutions using modified rice straw in a fixed bed column, Bioresour. Technol. 146 (2013) 519–524.

[5] B.A. Shah, C.B. Mistry, A.V. Shah, Sequestration of Cu(II) and Ni(II) from wastewater by synthesized zeolitic materials: Equilibrium, kinetics and column dynamics, Chem. Eng. J. 220 (2013) 172–184.

[6] M.A.S.D. Barros, E.A. Silva, P.A. Arroyo, C.R.G. Tavares, R.M. Schneider, M. Suszek, E.F. Sousa-Aguiar, Removal of Cr(III) in the fixed bed column and batch reactors using as adsorbent zeolite NaX, Chem. Eng. Sci. 59 (2004) 5959–5966.

[7] M. Jain, V.K. Garg, K. Kadirvelu, Cadmium(II) sorption and desorption in a fixed bed column using sunflower waste carbon calcium-alginate beads, Bioresour. Technol. 129 (2013) 242–248.

[8] Y. Long, D. Lei, J. Ni, Z. Ren, C. Chen, H. Xu, Packed bed column studies on lead(II) removal from industrial wastewater by modified *Agaricus bisporus*, Bioresour. Technol. 152 (2014) 457–463.

[9] T. Nur, W.G. Shim, M.A.H. Johir, S. Vigneswaran, J. Kandasami, Modelling of phosphorus removal by ion-exchange resin (Purolite FerrIX A33E) in fixed-bed column experiments, Desalin. Water Treat. (2013) 1–7.

[10] M. López-García, P. Lodeiro, R. Herrero, J.L. Barriada, C. Rey-Castro, C. David, M.E. Sastre de Vicente, Experimental evidences for a new model in the description of the adsorption-coupled reduction of Cr(VI) by protonated banana skin, Bioresour. Technol. 139 (2013) 181–189.

[11] J. Samuel, M. Pulimi, M.L. Paul, A. Maurya, N. Chandrasekaran, A. Mukherjee, Batch and continuous flow studies of adsorptive removal of Cr(VI) by adapted bacterial consortia immobilized in alginate beads, Bioresour. Technol. 128 (2013) 423–430.

[12] O. Hamdaoui, Removal of copper(II) from aqueous phase by Purolite C100-MB cation exchenge resin in fixed bed columns: Modeling, J. Hazard. Mater. 161 (2009) 737–746.

[13] S. Gupta, B.V. Babu, Modeling, simulation, and experimental validation for continuous Cr(VI) removal from aqueous solutions using sawdust as an adsorbent, Bioresour. Technol. 100 (2009) 5633–5640.

[14] H. Ye, Q. Zhu, D. Du, Adsorptive removal of Cd(II) from aqueous solution using natural and modified rice husk, Bioresour. Technol. 101 (2010) 5175–5179.

[15] A.A. Hekmatzadeh, A. Karimi-Jashni, N. Talebbeydokhti, B. Kløve, Modeling of nitrate removal for ion exchange resin in batch and fixed bed experiments, Desalination 284 (2011) 22–31.

[16] M. Izquierdo, C. Gabaldón, P. Marzal, F.J. Álvarez-Hornos, Modeling of copper fixed-bed biosorption from wastewater by *Posidonia oceanica*, Bioresour. Technol. 101 (2010) 510–517.

[17] D. Peaceman, Fundamental of Numerical Reservoir Simulation, Elsevier Scientific Publication Co., Amsterdam, 1977.

[18] N.K. Hiester, T. Vermeulen, Saturation performance of ion -exchange and adsorption columns, Chem. Eng. Prog. 48 (1952) 505–516.

[19] H.C. Thomas, Heterogeneous ion exchange in a flowing system, J. Am. Chem. Soc. 66 (1944) 1664–1666.

[20] M.A. Hashim, K.H. Chu, Prediction of protein breakthrough behavior using simplified analytical solutions, Sep. Purif. Technol. 53 (2007) 189–197.

[21] A.P. Lim, A.Z. Aris, Continuous fixed-bed column study and adsorption modeling: Removal of cadmium (II) and lead(II) ions in aqueous solution by dead calcareous skeletons, Biochem. Eng. J. 87 (2014) 50–61.

[22] İ.Y. İpek, N. Kabay, M. Yüksel, Modeling of fixed bed column studies for removal of boron from geothermal water by selective chelating ion exchange resins, Desalination 310 (2013) 151–157.

[23] E.L. Cochrane, S. Lu, S.W. Gibb, I. Villaescusa, A comparison of low-cost biosorbents and commercial sorbents for the removal of copper from aqueous media, J. Hazard. Mater. B 137 (2006) 198–206.

[24] S. Svilović, D. Rušić, R. Stipišić, Modeling batch kinetics of copper ions sorption using synthetic zeolite NaX, J. Hazard. Mater. 170 (2009) 941–947.

[25] M. Calero, F. Hernáinz, G. Blázquez, G. Tenorio, M.A. Martín-Lara, Study of Cr(III) biosorption in a fixed-bed column, J. Hazard. Mater. 171 (2009) 886–893.

[26] E.I. Unuabonah, B.I. Olu-Owolabi, E.I. Fasuyi, K.O. Adebowale, Modeling of fixed-bed column studies for the adsorption of cadmium onto novel polymer-clay composite adsorbent, J. Hazard. Mater. 179 (2010) 415–423.

[27] M.K. Mondal, Removal of Pb(II) ions from aqueous solution using activated tea waste: Adsorption on a fixed-bed column, J. Environ. Manage. 90 (2009) 3266–3271.

[28] S. Chen, Q. Yue, B. Gao, Q. Li, X. Xu, K. Fu, Adsorption of hexavelent chromium from aqueous solution by modified corn stalk: A fixed-bed column study, Bioresour. Technol. 113 (2012) 114–120.

[29] W. Li, Q. Yue, P. Tu, Z. Ma, B. Gao, J. Li, , X. Xu, Adsorption characteristics of dyes in columns of activated carbon prepared from paper mill sewage sludge, Chem. Eng. J. 178 (2011) 197–203.

[30] N. Selvaraju, S. Pushpavanam, Adsorption characteristics on sand and brick beds, Chem. Eng. J. 147 (2009) 130–138.

[31] A. Sulaymon, K.W. Ahmed, Competitive adsorption of furfural and phenolic compounds onto activated carbon in fixed bed column, Environ. Sci. Technol. 42 (2008) 392–397.